Redistribution of brain glucose metabolism in people with HIV after antiretroviral therapy initiation

Zeping Wang[a], Maura M. Manion[b], Elizabeth Laidlaw[b], Adam Rupert[c], Chuen-Yen Lau[d], Bryan R. Smith[e], Avindra Nath[e], Irini Sereti[b] and Dima A. Hammoud[a]

See related paper on page 1309

Objective: We evaluated brain glucose metabolism in people living with HIV (PWH) with [^{18}F]-Fluoro-Deoxyglucose (FDG) PET/computed tomography (CT) before and after antiretroviral therapy (ART) initiation.

Design: We conducted a longitudinal study wherein ART-naive late-presenting untreated PWH with CD4$^+$ cell counts less than 100 cells/μl were prospectively assessed for FDG uptake at baseline and at 4–8 weeks ($n = 22$) and 19–26 months ($n = 11$) following ART initiation.

Methods: Relative uptake in the subcortical regions (caudate, putamen and thalamus) and cortical regions (frontal, parietal, temporal and occipital cortices) were compared across time and correlated with biomarkers of disease activity and inflammation, in addition to being compared with a group of uninfected individuals ($n = 10$).

Results: Before treatment initiation, putaminal and caudate relative FDG uptake values in PWH were significantly higher than in uninfected controls. Relative putaminal and thalamic uptake significantly decreased shortly following ART initiation, while frontal cortex values significantly increased. FDG uptake changes correlated with changes in CD4$^+$ cell counts and viral load, and, in the thalamus, with IL-6R and sCD14. Approximately 2 years following ART initiation, there was further decrease in subcortical relative uptake values, reaching levels below those of uninfected controls.

Conclusion: Our findings support pretreatment basal ganglia and thalamic neuroinflammatory changes in PWH, which decrease after treatment with eventual unmasking of long-term irreversible neuronal damage. Meanwhile, increased frontal cortex metabolism following ART initiation suggests reversible cortical dysfunction which improves with virologic control and increased CD4$^+$ cell counts. Early initiation of treatment after HIV diagnosis and secondary control of inflammation are thus necessary to halt neurological damage in PWH.

AIDS 2021, **35**:1209–1219

Keywords: brain metabolism, brain PET imaging, HIV, inflammation

[a]Center for Infectious Disease Imaging, Radiology and Imaging Sciences, Clinical Center, National Institutes of Health, [b]Laboratory of Immunoregulation, National Institute for Allergy and Infectious Diseases, National Institutes of Health, Bethesda, [c]Leidos Biomedical Research Inc., Frederick National Laboratory for Cancer Research, Frederick, [d]National Institute for Allergy and Infectious Diseases, National Institutes of Health, and [e]Section of Infections of the Nervous System, National Institute of Neurological Diseases and Stroke, Bethesda, Maryland, USA.

Correspondence to Dima A. Hammoud, MD, National Institutes of Health/Clinical Center, 10 Center Drive, Room 1C368, Bethesda, MD 20892, USA.

Tel: +1 301 402 3041; e-mail: hammoudd@cc.nih.gov
Received: 29 September 2020; revised: 12 February 2021; accepted: 19 February 2021.

DOI:10.1097/QAD.0000000000002875

Introduction

The introduction of combination antiretroviral therapy (cART) has greatly reduced the morbidity and mortality associated with HIV infection [1,2]. Despite these advances, rates of HIV-associated neurocognitive impairment remain high, with asymptomatic and mild neurocognitive impairment still reported to occur in around 30–50% of patients [3–6]. HIV enters the central nervous system (CNS) early in the course of infection [7] via infected monocytes and lymphocytes [3,8–10]. Once in the brain, HIV infection of macrophages, microglial cells and astrocytes leads to chronic inflammation, which is believed to be the primary source of neuronal damage in untreated people living with HIV (PWH) [3,11]. The pathophysiology of CNS disease in PWH after treatment, however, remains less well understood.

Although multiple studies have investigated neurocognition [1,2] and brain volumetric changes in treated PWH [12,13], few studies have focused on the acute and chronic effects of ART initiation from a metabolic perspective. Whether an inflammatory component of the infection is acutely detectable in the brains of infected patients, and how this inflammation is modified by effective ART, remains unclear. In this study, we aimed to better understand brain metabolic changes in a group of late-presenting ART-naive PWH patients with low $CD4^+$ cell counts [14], as it relates to ART initiation and maintenance. To assess glucose metabolism in the cortical and subcortical regions of the brain as a reflection of neuroinflammation and neuronal function, participants underwent ^{18}F-Fluorodeoxyglucose (FDG) PET/CT scans before and once ($n = 22$) or twice ($n = 11$) after initiation of ART (short and long-term follow-up). FDG uptake values from the baseline and long-term treated PWH scans were also compared with values obtained from a group of uninfected HIV-negative controls. Finally, we looked for associations between FDG uptake in PWH and biomarkers of disease activity and immune activation in the periphery, in an attempt to correlate changes in metabolic activity with overall disease progression.

Materials and methods

Study design

PWH and HIV-negative controls were recruited and scanned under protocols 14-I-0124 (PET Imaging and Lymph Node Assessment of IRIS in Persons With AIDS, PANDORA, NCT02147405) and 13-N-0149 (Screening and Recruitment for HIV-associated Neurocognitive Disorders Studies and an Evaluation of HIV-associated Neurocognitive Disorders in Virologically Controlled Patients, NCT01875588), respectively. Both studies were reviewed and approved by the National Institute of Allergy and Infectious Diseases Institutional Review Board and by the NIH Radiation Safety Committee in keeping with the Declaration of Helsinki of the World Medical Association. All participants signed informed consent before study procedures began.

This was a prospective observational study of 22 PWH. The PWH participants had $CD4^+$ T-cell counts of less than 100 cells/μl at baseline, were naive to ART and were willing to start therapy. ART was initiated according to standard treatment guidelines in all PWH, as part of enrolment in the NCT02147405 protocol, usually within 2 weeks after study enrolment. The choice of ART was based on each participant's genotype, comorbidities and possible drug interactions. Changes in ART during the disease course were dictated by response criteria and side effects. Only PWH with no evidence of active CNS opportunistic infection or CNS immune reconstitution inflammatory syndrome (IRIS) were included in this sub-study [15]. Ten seronegative controls were selected from the neurocognitive disorders study (NCT01875588), which recruited uninfected controls from the DC metro area to match age, sex and social history of the enrolled PWH [16].

FDG-PET/computed tomography imaging

FDG PET/CT scans for the 22 PWH participants were performed prior to ART initiation and 4–8 weeks after ART initiation (short-term ART) using a clinical PET/CT scanner (Biograph PET/CT; Siemens Medical Solutions, Malvern, Pennsylvania, USA). A subset of 11 PWH participants received an additional FDG PET/CT scan 19–26 months following ART initiation (long-term ART). All participants consented to undergoing FDG PET/CT for research purposes.

Approximately 58 min following the injection of 10 mCi of ^{18}F-FDG, each PWH was positioned on the scanner table and a low-dose CT scan was performed from the top to the base of the skull for attenuation correction and anatomical localization under protocol 14-I-0124, NCT02147405. Emission scans were then obtained in three-dimensional mode for a duration of 10–15 min. Images were reconstructed with an iterative technique featuring an ordered subset expectation-maximization algorithm and attenuation and scatter corrected with a CT-based correction. The 10 controls were imaged on the same PET/CT scanner with the same acquisition and reconstruction techniques following the administration of 5 mCi of ^{18}F-FDG (scanned under protocol 13-N-0149, NCT01875588). The differences in doses are due to the different objectives of the two studies, which included whole body scanning (including the brain) for NCT02147405 compared with only brain imaging in NCT01875588.

Quantification analysis of subcortical and cortical FDG uptake

FDG uptake (whole-brain and brain region specific) was assessed using the Neuro Tool in PMOD version 4.002 (PMOD Technologies LC, Zurich, Switzerland).

Standardized uptake values (SUVs) for the basal ganglia (caudate and putamen), thalamus and whole brain were generated through application of automatic template volumes of interest (VOIs) to each PET scan. The subcortical VOIs were manually adjusted as needed. The right and left VOIs of each structure (caudate, putamen and thalamus) were merged and SUVmean values were obtained for the merged VOI. Regional VOIs for the frontal, parietal, temporal and occipital cortical regions were similarly generated using the Neuro Tool in PMOD. The left and right cortical subregions were fused together and SUVmean values were then calculated. We evaluated all the regions by averaging the right and left hemispheres in order to decrease the probability of type 1 statistical errors due to multiple comparisons.

Partial volume correction (PVC) calculations were applied to each of the VOIs from the three subcortical structures and four cortical regions using VOI-based algorithms [17,18]. Relative uptake was then calculated as a ratio of each structure's regional uptake to the whole brain uptake. We used relative SUV values as those have been proven to be more stable quantitative indices of cerebral glucose metabolism than absolute SUV values [19], and because control participants had received a lower FDG dose.

Peripheral disease markers

$CD4^+$ cell counts and plasma viral load values were measured at each imaging time point for all 22 PWH participants. For 15 of the 22 PWH, cryopreserved plasma was obtained within one week of the baseline, short-term and long-term follow-up FDG-PET scans. Samples were analysed by ELISA on a VIDAS instrument for D-dimer (bioMerieux Inc., Durham, North Carolina, USA) and by ELISA kits (R&D Systems, Minneapolis, Minnesota, USA and MyBiosource.com, San Diego, California, USA) for sCD14. Plasma levels of IFN-γ [lower limit of detection (LLD) = 0.40 pg/ml], TNF-α (LLD = 0.09 pg/ml), MPO (LLD = 0.07 ng/ml), MCP-1 (LLD = 0.11 pg/ml), sPD1 (LLD = 0.00 pg/ml), sCD14 (LLD = 2.5 E-7 mg/l), IL-2 (LLD = 0.38 pg/ml), IL-6 (LLD = 0.18 pg/ml), IL-8 (LLD = 0.16 pg/ml), IL-10 (LLD = 0.09 pg/ml), IL-6R (LLD = 0.49 pg/ml) and G-CSF (LLD = 0.24 pg/ml) were measured using a custom multiplex kit and three single-plex kits by electrochemiluminescence (Meso Scale Discovery, Gaithersburg, Maryland, USA). Results from IL-1b and IL-12p70 were at or below LLD and were excluded.

Statistical methods

Shapiro–Wilk normality tests were applied to all data sets before statistical analyses were conducted between groups. Due to nonnormal distributions in a few data sets, nonparametric tests were used for all analyses to maintain consistency. Nonparametric tests are typically more conservative than parametric tests and would not be expected to increase type I error. Values deemed to be outliers using the Grubb's method were excluded.

Comparisons for relative FDG uptake changes in the short term (baseline and short-term ART; $n = 22$) were assessed for both the cortical (composite of all regions of cortex) and subcortical (caudate, putamen and thalamus) regions. Comparisons of the two groups were performed using Wilcoxon tests (matched-pairs signed rank tests). The statistical significance criteria for these comparisons were set to P value less than 0.05.

Changes in FDG uptake across the long-term scans (baseline, short-term ART and long-term ART; $n = 11$) were assessed for the cortical and subcortical regions using Friedman tests (nonparametric repeated-measures one-way ANOVA). Following nonparametric ANOVA analysis, Dunn's multiple comparison tests for differences between each of the three time points were further conducted, if warranted. The statistical significance criteria for these comparisons were set to P value less than 0.05.

Relative FDG uptake values of PWH's brain regions from the baseline ($n = 22$) and long-term ART time points ($n = 11$) were separately compared to corresponding cortical and subcortical measurements from control participants ($n = 10$) using Mann–Whitney tests (nonparametric unpaired t-tests). The criteria for statistical significance for these analyses were set to P value less than 0.05.

Within individual PWH participants, $CD4^+$ cell counts and plasma viral load values were correlated with relative FDG uptake values at different time points using repeated measures correlations [20] for both the short-term ($n = 22$) and long-term ART ($n = 11$) time points. Additional markers of immune activation and inflammation that were available were correlated with subcortical and cortical uptake values between baseline and short-term ART follow-up ($n = 15$). At the long-term ART time point, correlations with soluble biomarkers were not performed, as a complete data set of biomarkers was only available for seven patients. Correlations were performed using the *rmcorr* program in R (version 3.5.1; R Foundation, Vienna, Austria), with statistical significance set to P value less than 0.01 due to multiple correlations.

Data availability statement

Anonymized data not published within this article will be made available by request from any qualified investigator.

Results

Clinical characteristics of study participants

Twenty-two ART-naive, PWH participants [six women and 16 men; median age, 36.6 years (interquartile range, IQR, 32.2–39.9], were recruited from the greater

Washington, DC area and their HIV clinical care was provided through protocol participation at the National Institutes of Health, Clinical Center (Supplemental Table S1, http://links.lww.com/QAD/C67). Participants had nadir $CD4^+$ cell counts ranging from 0 to 84 cells/μL [median count, 26.0 (IQR, 10–41.3)]. Ten uninfected control participants [median age, 53.7 (IQR, 50.1–56.5)] were included in the study.

Six of the 22 PWH were eventually diagnosed with non-CNS IRIS based on AIDS Clinical Trial Group criteria (https://actgnet-work.org/IRIS_case_definitions). IRIS developed within 1–12 weeks of starting ART [median weeks, 3 (IQR, 2–8)]. Among those, four participants were already diagnosed with IRIS when they underwent their short-term F/U scans, while two had not been diagnosed with IRIS yet. Three individuals were on corticosteroids at the time of the first scan, while the other three had stopped the corticosteroids prior to the PET scan. None of the participants had evidence of opportunistic CNS infection. In one (#6), there was history of shingles prior to presentation and the CSF was positive for varicella zoster virus (VZV) by PCR. This was, however, considered not to be indicative of opportunistic CNS infection as both the CSF profile (WBC: 3 leukocytes/μl, protein: 34 mg/dl, glucose: 70 mg/dl) and the enhanced brain MRI and MRA were normal. All participants experienced increases in $CD4^+$ cell counts and decreases in plasma HIV viremia by the time the second FDG-PET was performed. All 11 PWH participants with a long-term follow-up scan were virally suppressed with viral load less than 40 copies at the third time point. A table showing the clinical characteristics of all PWH participants is included (Table S1, http://links.lww.com/QAD/C67).

There were significant increases in $CD4^+$ cell counts and decreases in plasma viral load across all time points for the PWH patients. Baseline values were significantly different in the 22 participants compared with their short-term ART follow-up ($P < 0.0001$ for $CD4^+$ cell count and $P < 0.0001$ for viral load) (Fig. S1-A, http://links.lww.com/QAD/C64). $CD4^+$ cell counts in the long-term group ($n = 11$) significantly increased between baseline and long-term post-ART ($P < 0.0001$); their plasma viral load levels first decreased significantly in the short term ($P = 0.012$) and decreased further in the long term ($P < 0.0001$). All viral load values dropped below the level of detection by the last time point (Fig. S1-B, http://links.lww.com/QAD/C64).

Whole-brain FDG uptake

There were no significant differences in whole brain SUVmean values across all three time points (long-term ART; $n = 11$) or across two time points (short-term ART; $n = 22$).

Subcortical and cortical FDG uptake

In the putamen, relative SUV (rSUV) values decreased significantly at short-term follow-up after ART initiation (Wilcoxon test, $P < 0.0001$) (Fig. 1a). When the long-term scans were added to the analysis, the significant differences persisted (Friedman test, $P = 0.002$) (Fig. 1b). Posthoc analysis showed a significant decrease in the short-term compared to baseline ($P = 0.032$) as well as in the long-term compared with baseline ($P = 0.004$),

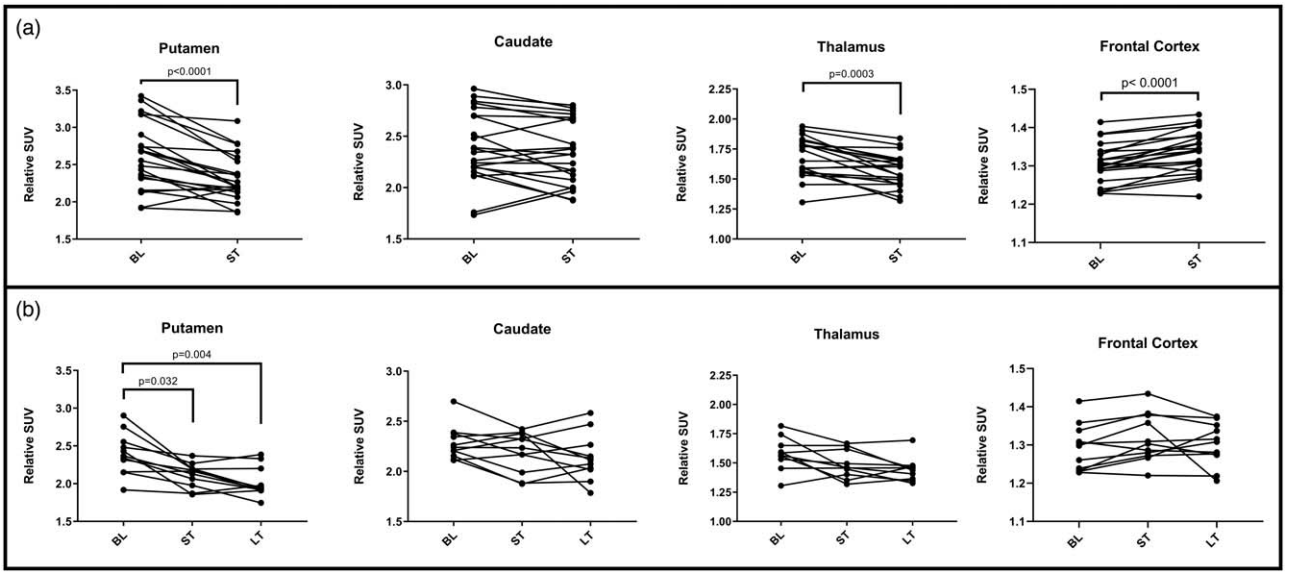

Fig. 1. Longitudinal changes in relative standardized uptake value in the caudate, putamen, thalamus and frontal cortex between the baseline, short-term follow-up (ST, $n = 22$) (a) and long-term follow-up after ART initiation (LT, n = 11) (b). For the thalamic dataset, one individual was excluded as an outlier.

although there were no significant differences between the short and long-term values.

In the caudate, the mean and median of the rSUV values decreased between baseline and both short-term and long-term ART time-points. These differences, however, were not statistically significant (Fig. 1a, b).

In the thalamus, one participant's values had to be excluded (outlier as determined by Grubb's method). Only short-term comparisons were significant with decreased rSUV values ($P = 0.0003$) compared with baseline (Fig. 1A). There were no significant differences when all three time-points were analysed together (Fig. 1b).

For the cortical VOIs ($n = 22$), the frontal cortex rSUV significantly increased from baseline to short-term post-ART (Wilcoxon test, $P < 0.0001$) (Fig. 1a). There were no significant differences in rSUV for any of the other evaluated cortical regions. When long-term scans were included ($n = 11$), there were no significant differences in uptake across the three time points in any cortical region, including the frontal cortex (Fig. 1b).

In patients who developed systemic IRIS, the median values for rSUV were higher in the subcortical regions and in the frontal cortex compared to those who did not develop IRIS, more so at baseline than at later time points. The differences between IRIS and non-IRIS participants however did not reach statistical significance in any of the regions, at any of the time points (Mann–Whitney, $P > 0.05$) (Fig. S2, http://links.lww.com/QAD/C65).

Each of the regions had a few patients that showed an increase in rSUV between the pre-ART and one or both ART time-points. They were mostly non-IRIS patients and a review of their ART regimens revealed no obvious differences when compared to patients with decreased rSUV values.

When the patients were separated by sex, there were also no statistically significant differences in rSUV values between men and women in any region at any time point (Fig. S3, http://links.lww.com/QAD/C66).

FDG uptake in people living with HIV before antiretroviral therapy and following long-term antiretroviral therapy in comparison to controls

At baseline, ART-naive PWH participants showed significantly higher rSUV values in the putamen when compared to uninfected controls ($P = 0.005$). Relative FDG uptake values in the caudate were also higher in PWH participants, but with only borderline significance ($P = 0.025$). In the thalamus, the differences did not reach statistical significance. Cortical rSUV values in PWH were also not significantly different from uptake values in controls (Fig. 2a).

However, when comparing the long-term rSUV values to control values ($n = 11$), a reversed pattern was observed with significantly lower relative uptake in the thalamus

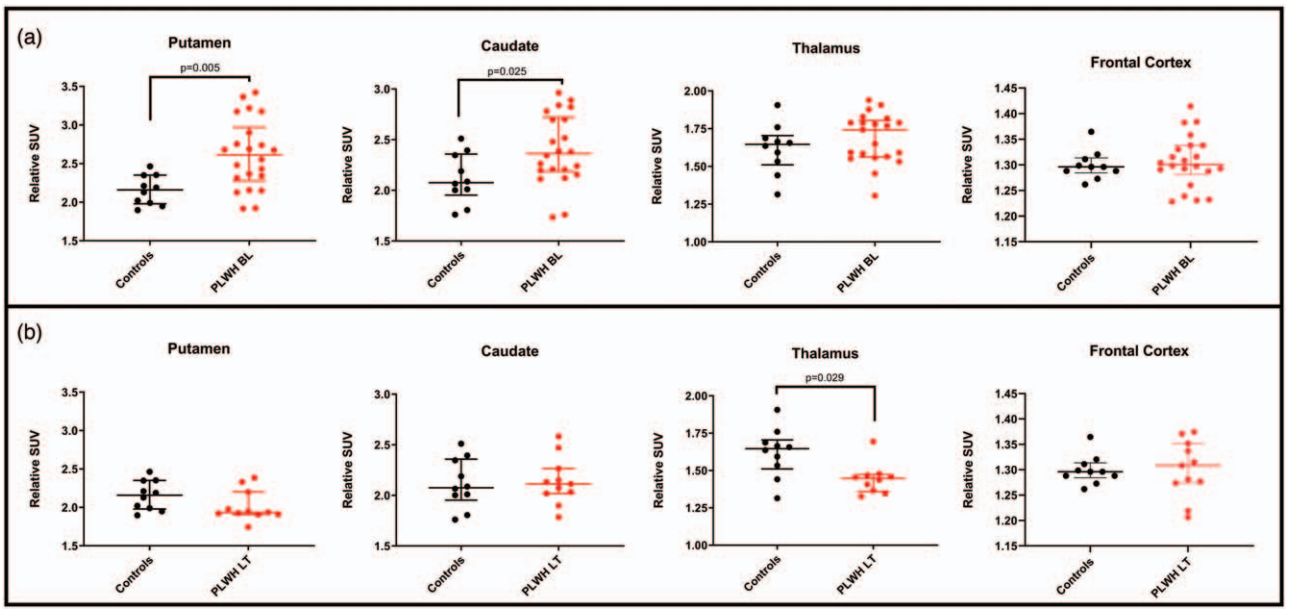

Fig. 2. (a) Differences in relative standardized uptake value in the putamen, caudate, thalamus and frontal cortex between ART-naive PWH at baseline (BL < $n = 22$) and uninfected controls ($n = 10$). (b) Differences in relative SUV in the caudate, putamen, thalamus and frontal cortex between PWH on continuous long-term ART for approximately 2 years (LT, $n = 11$) and uninfected controls ($n = 10$). For the thalamic dataset, one individual was excluded as an outlier.

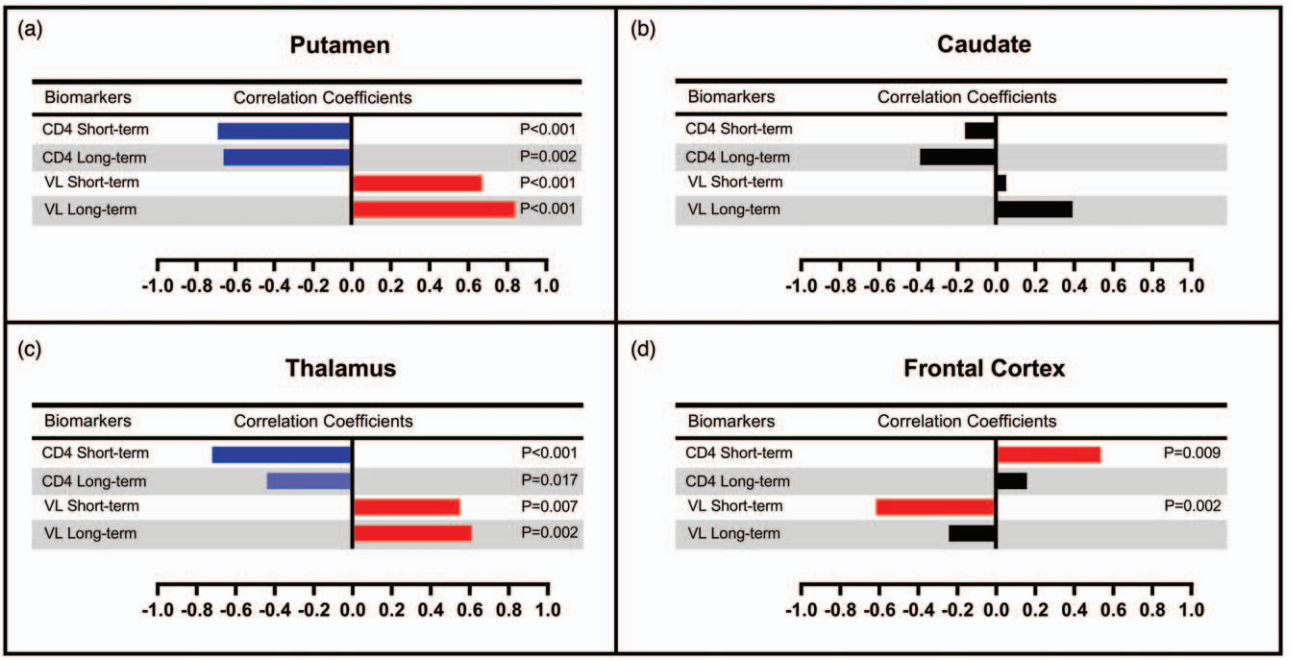

Fig. 3. Repeated measures correlations between regional relative standardized uptake value values and CD4$^+$ cell counts/ plasma viral loads in the short-term (ST, $n = 22$) and long-term (LT, $n = 11$) follow-up after ART initiation.

($P = 0.029$). The other regions were not significantly different in rSUV between PWH and controls (Fig. 2b).

Correlations of regional uptake with peripheral viremia and CD4$^+$ cell counts

Repeated measures correlations from the first two time points (baseline and short-term ART; $n = 22$) showed a significant negative association between rSUV values of the putamen and CD4$^+$ cell counts ($P = 0.0003$, $r = -0.69$) and a significant positive association with viral load ($P = 0.0005$, $r = 0.67$) (Fig. 3a). No significant correlations were found for the caudate rSUV with CD4$^+$ cell counts or viral load (Fig. 3b). Similar to the putamen results, the thalamic rSUV values showed a significant negative correlation with CD4$^+$ cell counts ($P = 0.0001$, $r = -0.72$) and a significant positive correlation with viral load ($P = 0.007$, $r = 0.55$) (Fig. 3c). Frontal and temporal cortical rSUV values had significant positive correlations with CD4$^+$ cell counts ($P = 0.009$, $r = 0.54$ and $P = 0.007$, $r = 0.55$, respectively), while frontal lobe rSUV values had a significantly negative correlation with viral load ($P = 0.002$, $r = -0.62$) (Fig. 3d). Cortical associations were opposite in direction to subcortical regional correlations.

In the long-term ART group ($n = 11$), putaminal rSUV values remained positively associated with viral load ($P < 0.0001$, $r = 0.84$) and negatively associated with CD4$^+$ cell count ($P = 0.0006$, $r = -0.66$) (Fig. 3a). Thalamic rSUV remained positively associated with viral load ($P = 0.002$, $r = 0.61$) with a negative trend association with CD4$^+$ cell counts ($P = 0.035$, $r = -0.44$) (Fig. 3c). The caudate and frontal cortex showed no significant correlations with either CD4$^+$ cell count or viral load.

Correlations of regional uptake with inflammatory biomarkers

In the longitudinal analyses, repeated measures correlations from the baseline and short-term follow-up revealed that relative uptake in the putamen and caudate showed a trend for positive correlations with various biomarkers (e.g. sIL-6R, sCD14 and D-dimer) (Fig. 4a, b). On the other hand, rSUV values in the thalamus significantly positively correlated with sIL-6R ($P = 0.0096$, $r = 0.63$) and sCD14 ($P = 0.007$, $r = 0.64$) (Fig. 4c). The frontal cortex was the only region showing a negative correlation with sCD14 ($P = 0.004$, $r = -0.68$), and a trend for significant negative correlations with sIL-6R ($P = 0.031$, $r = -0.54$) suggesting that uptake values increased as sCD14 and sIL-6R values in the periphery decreased (Fig. 4d).

Discussion

The exact pathophysiology of brain involvement with HIV infection in the acute and chronic stages remains unclear. In this study, using a longitudinal assessment of glucose metabolism in the brains of ART-naive PWH who were late-presenters, we were able to delineate the temporal progression of cortical and subcortical glucose

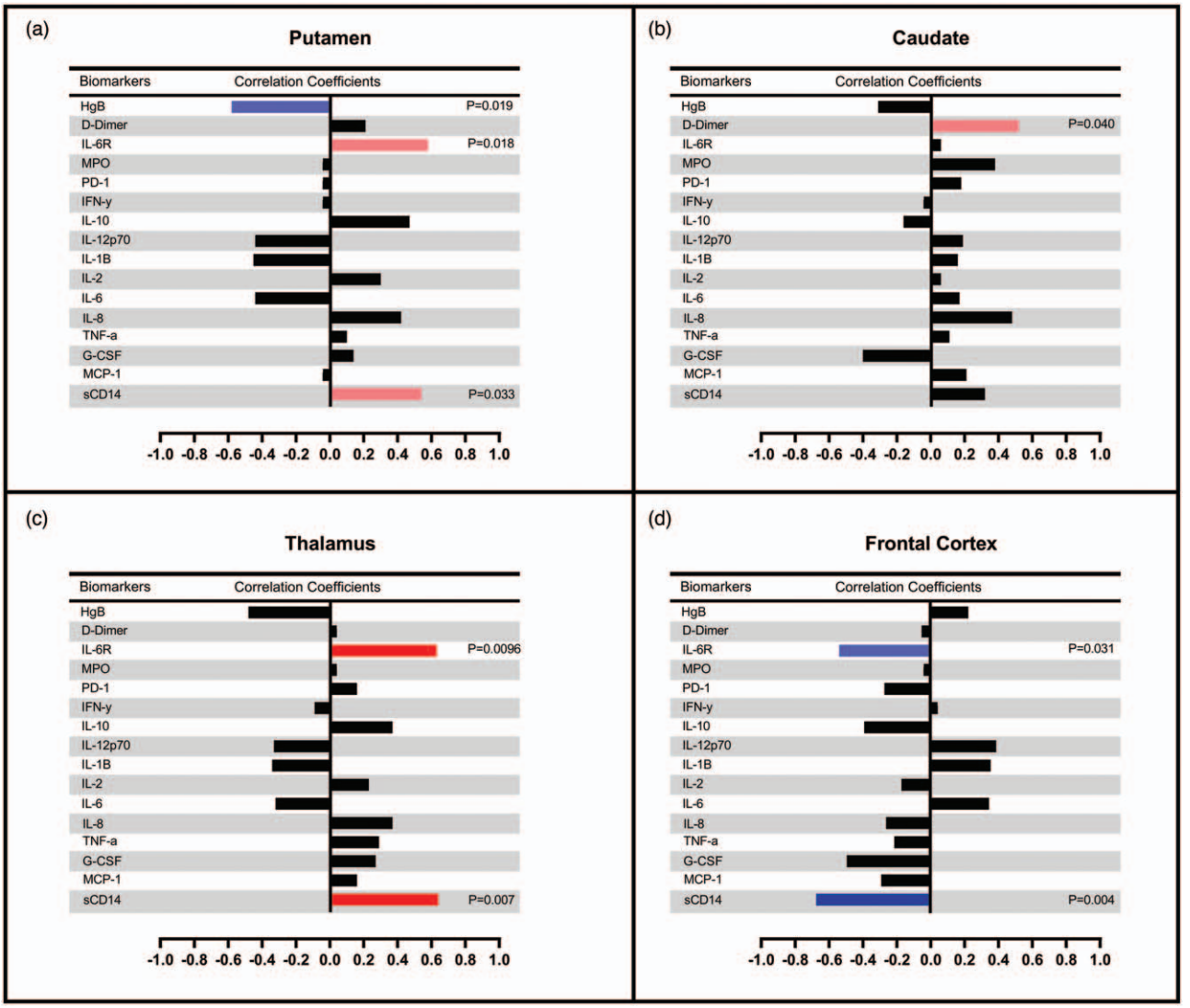

Fig. 4. Repeated measures correlations between relative standardized uptake value values and inflammatory markers in the short-term (ST, $n = 15$) follow-up after ART initiation.

metabolism changes associated with treatment. At baseline, basal ganglia and thalamic hypermetabolism in PWH compared with uninfected controls dominated the picture, especially in the putamen. Those changes, however, reversed promptly after initiation of ART, with decreased relative uptake, suggesting a baseline subcortical inflammatory process in association with HIV infection [3,21,22] that quickly decreases with peripheral control of the infection (Figs. 1 and 5). This was further supported with relative uptake values in the putamen and thalamus showing significant negative correlations with $CD4^+$ cell counts and significant positive correlations with plasma viral load values. This reduction of neuroinflammation also occurred in concert with decreasing inflammatory markers, leading to thalamic relative glucose metabolism correlating positively with sIL-6R and, more importantly, sCD14. The latter is a monocyte activation marker [23–25] known to persist even in early treated PWH [26] and to independently predict mortality in PWH [27]. In fact, a relationship between elevated sCD14 and brain HIV involvement has been previously proposed with higher levels being associated with worse cognitive performance [28–31].

Meanwhile, relative uptake in the frontal cortex increased following ART initiation (Fig. 5). The literature on FDG uptake in the cortical regions of PWH is scarce. MRI studies have provided insight into cortical involvement, with cortical thinning seen in the pre-ART stages of infection being halted following ART initiation [32]. Our FDG uptake findings in the frontal cortex at baseline could reflect neuronal injury and/or stunting in the setting of active viral replication. Increased relative uptake values after ART, however, suggests a reversible process with apparent rescuing of cortical activity, occurring in concert with increasing $CD4^+$ cell counts and decreasing

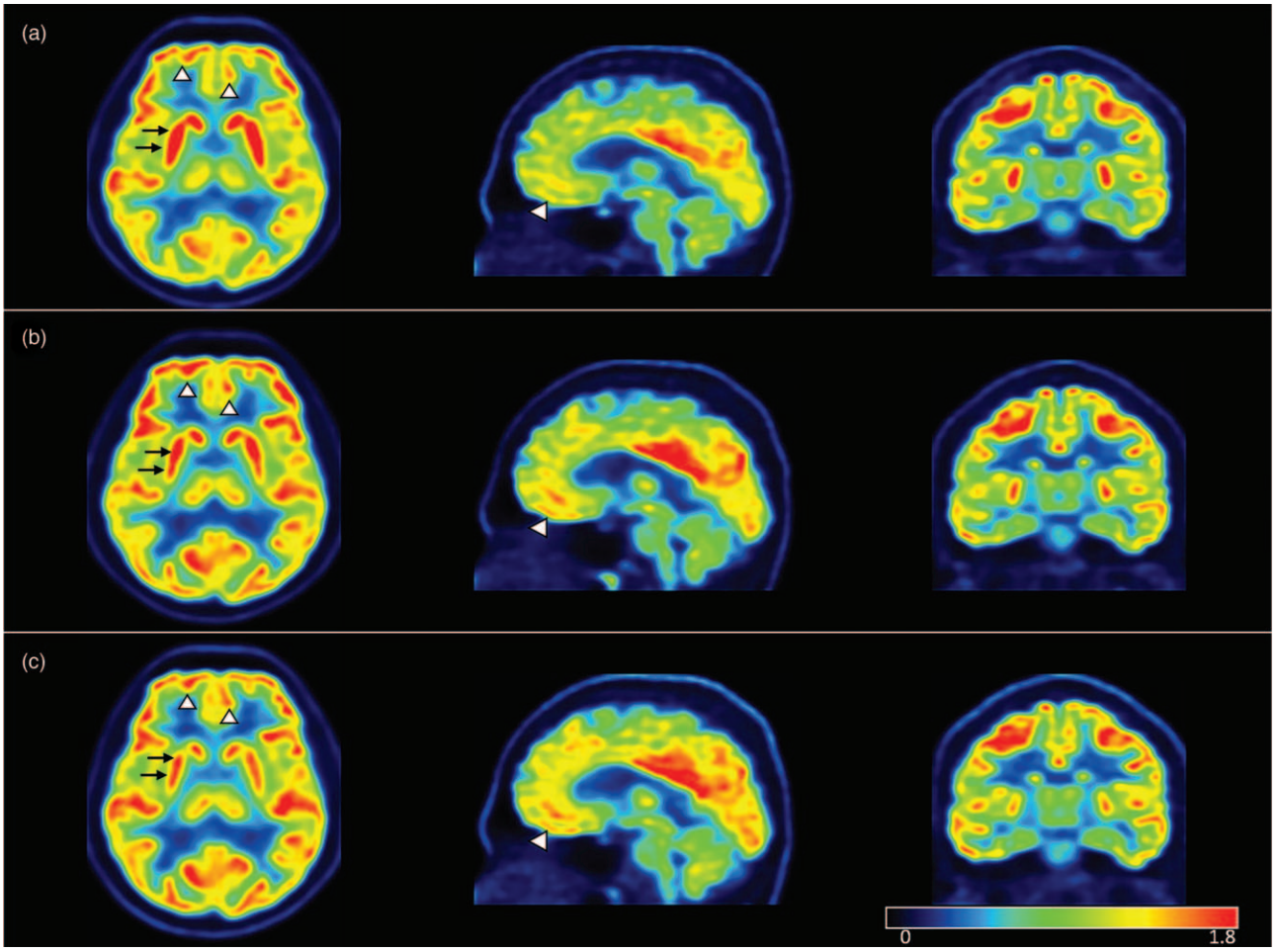

Fig. 5. Relative standardized uptake value parametric maps in one participant at (a) baseline, (b) short-term follow-up and (c) long-term follow-up. Axial, sagittal and coronal maps showing visually detectable decreasing putaminal (black arrows) and increasing cortical uptake (arrowheads) after initiation of ART.

viral load and sCD14 levels. As such, our findings suggest a better functional outcome in the frontal cortex following ART initiation than what has been established by structural imaging.

We also evaluated a subset of patients who were imaged after approximately two years of uninterrupted ART and found evidence for differential long-term injury in various brain regions: subcortical hypometabolism further progressed in the basal ganglia and thalamus, suggesting an element of irreversible injury and neuronal loss [13,33–35], while cortical metabolism did not change appreciably. With the limitations of a small sample number, our findings could reflect higher susceptibility of the thalamus and subcortical regions to the effects of the virus compared to the more resilient cortical structures. These findings are in concordance with multiple prior MR volumetric studies repeatedly demonstrating volume loss in subcortical structures [12,13,18]. In one of those studies, striatal volume loss was noted despite immediate initiation of ART in the acute stage of infection [18]. The exact reason for relative sparing of cortical neurons from permanent damage compared to subcortical neurons is unclear. Neuronal damage in the pretreatment stage, however, is likely due to a combination of viral protein toxicity, loss of astrocytic support, and neuroinflammatory changes with cytokine/chemokine release. A predilection for viral replication in the subcortical regions compared to cortical regions could thus exacerbate those effects and lead to subcortical/cortical dissociation as far as neurological damage. This predilection has been shown in brain autopsies of HIV-infected patients, with HIV-associated brain lesions identified mainly in the putamen and thalamus [36], as well as a higher concentration of HIV p24 positive cells in the basal ganglia [37]. We have also previously shown subcortical dopaminergic loss (both presynaptic and postsynaptic) in an animal model of HIV infection [38–41], which was associated with Gp120 levels and oxidative stress [39]. The exact underlying causes for subcortical predilection of damage in HIV are unclear. Prior studies of SIV-infected animals have demonstrated an association between increased

dopamine levels and CNS vacuolization, SIV encephalitic lesions and enhanced CNS viral replication during early infection [42,43]. This could be due to the role of dopamine in increasing the susceptibility of primary human macrophages to HIV entry through stimulation of both D1-like and D2-like receptors [44] via an alternative signalling pathway [45]. The abundance of dopaminergic neurons/projections in the basal ganglia, and to a lesser extent in the thalami and frontal cortex, could therefore possibly explain higher levels of viral replication in these regions compared to other regions.

In the pre-ART era, there were reports of initial hypermetabolism in the striatum in the acute and subacute stages of the infection and hypometabolism in the chronic stage [46–49]. The strength of our study, however, is in the longitudinal design and long-term follow-up scan. This allowed us to separate the rapid changes occurring shortly after ART initiation (decreased subcortical and increased cortical metabolism) from long-term changes (further subcortical hypometabolism probably due to neuronal loss). While the former effect is likely due to decreased neuroinflammation, the latter is more likely to reflect long-term neuronal loss.

Despite the limitations of spatial resolution associated with PET, this modality has the advantage of very high sensitivity compared to MRI as well as the ability to surpass structural abnormalities and detect subtle functional and molecular changes. Although FDG PET is widely available as a clinical tool, the associated radiation limits its applicability in evaluating individual patients. The information obtained from group analysis, however, such as in our study, can shed light on the pathophysiology of disease involvement, beyond what can be derived from structural imaging modalities and neurocognitive testing alone.

A limitation of our study is the small sample size of our long-term cohort. A larger sample size could have resulted in better appreciation of subtle changes in metabolism in various regions and could have allowed us to better assess the contribution of various factors such as HIV clade, substance use and comorbidities to the end result of neuronal dysfunction/loss. Another limitation is a significantly older control group. This, however, further supports our results of abnormally decreased metabolism in PWH since one would expect an older population to have shown lower glucose metabolism values [50]. Additional limitations include the lack of CSF measurements, including inflammatory or neuronal injury biomarkers, the lack of plasma ART levels and the partial availability of plasma biomarkers. As all PWH participants achieved appropriate plasma virologic suppression, however, we do not believe variability in drug levels would have played a major role in their FDG findings. There was a difference in injected FDG dose between PWH and controls, as the two groups were scanned under different protocols. However, this should not affect our results, as we used SUV values (which account for the injected dose and body weight) and because we relied on comparisons between relative SUV values (which normalize regional uptake to whole brain uptake) rather than absolute SUV values. Finally, our PWH population consisted of late-presenters with low nadir $CD4^+$ cell count (<100 cells/μl at baseline). This could have magnified the neuroinflammatory and eventual neurodegenerative changes compared to PWH with higher $CD4^+$ cell counts upon presentation, which would be consistent with previous observations showing low $CD4^+$ cell count nadir as a predictor of HIV neurocognitive impairment [51]. Late-presenters, however, still constitute a large proportion of PWH starting therapy, especially in resource-limited settings. Our advanced imaging techniques are not readily available in such settings due to infrastructure, expertise and financial constraints. As a result, we believe the information we are gleaning regarding the neuropathophysiology of the infection in this study using FDG PET imaging will eventually inform and improve the management of late-presenters in countries with limited resources, especially as it relates to CNS manifestations in those patients.

In summary, our findings suggest that there is differential regional susceptibility of the brain to HIV infection with maximal effects in the basal ganglia, particularly the putamen, and the thalamus. ART has a significant role in tempering neuroinflammatory changes in the brain in concert with the abatement of systemic viral replication and inflammation. Long-term subcortical decreases in glucose metabolism, on the other hand, are likely the result of irreversible neuronal damage associated with pretreatment neuroinflammatory changes, although other factors, including ART toxicity [52,53] and cardiovascular disease [16], cannot be ruled out. Our findings support the importance of early initiation of treatment and controlling viral replication/neuroinflammation in minimizing neurological damage, and suggest that FDG PET may be a sensitive technique for monitoring the effects of ART in this population.

Acknowledgements

This work was supported entirely by the Intramural Research Programs of the Clinical Center (CC), National Institute of Neurological Diseases and Stroke (NINDS), and National Institute for Allergy and Infectious Diseases (NIAID), National Institutes of Health (NIH), Bethesda, Maryland, USA.

D.A.H., B.R.S., A.N. and I.S. conceived of and designed the study; Z.W., M.M.M., E.L., A.R., C.-Y.L., B.R.S., A.N., I.S. and D.A.H. evaluated the study individuals and/or collected and analysed the data; Z.W. performed the statistical analysis. All authors participated in drafting

the article and/or revising it critically for intellectual content, and gave final approval of the submitted manuscript.

Conflicts of interest

Z.W., M.M.M., E.L., A.R., C.-Y.L., B.R.S., A.N., I.S. and D.A.H. report no disclosures. There are no conflicts of interest.

References

1. Heaton RK, Clifford DB, Franklin DR Jr, Woods SP, Ake C, Vaida F, *et al*. **HIV-associated neurocognitive disorders persist in the era of potent antiretroviral therapy: CHARTER Study.** *Neurology* 2010; **75**:2087–2096.
2. Heaton RK, Franklin DR, Ellis RJ, McCutchan JA, Letendre SL, Leblanc S, *et al*. **HIV-associated neurocognitive disorders before and during the era of combination antiretroviral therapy: differences in rates, nature, and predictors.** *J Neurovirol* 2011; **17**:3–16.
3. Schouten J, Cinque P, Gisslen M, Reiss P, Portegies P. **HIV-1 infection and cognitive impairment in the cART era: a review.** *Aids* 2011; **25**:561–575.
4. Sheppard DP, Iudicello JE, Morgan EE, Kamat R, Clark LR, Avci G, *et al*. **Accelerated and accentuated neurocognitive aging in HIV infection.** *J Neurovirol* 2017; **23**:492–500.
5. Saloner R, Campbell LM, Serrano V, Montoya JL, Pasipanodya E, Paolillo EW, *et al*. **Neurocognitive SuperAging in older adults living with HIV: demographic, neuromedical and everyday functioning correlates.** *J Int Neuropsychol Soc* 2019; **25**:507–519.
6. Portilla I, Reus S, León R, van-der Hofstadt C, Sánchez J, López N, *et al*. **Neurocognitive impairment in well controlled HIV-infected patients: a cross-sectional study.** *AIDS Res Hum Retroviruses* 2019; **35**:634–641.
7. Thurnher MM, Donovan Post MJ. **Neuroimaging in the brain in HIV-1-infected patients.** *Neuroimaging Clin N Am* 2008; **18**:93–117viii.
8. Ho EL, Ronquillo R, Altmeppen H, Spudich SS, Price RW, Sinclair E. **Cellular composition of cerebrospinal fluid in HIV-1 infected and uninfected subjects.** *PLoS One* 2013; **8**:e66188.
9. Zayyad Z, Spudich S. **Neuropathogenesis of HIV: from initial neuroinvasion to HIV-associated neurocognitive disorder (HAND).** *Curr HIV/AIDS Rep* 2015; **12**:16–24.
10. Subra C, Trautmann L. **Role of T lymphocytes in HIV neuropathogenesis.** *Curr HIV/AIDS Rep* 2019; **16**:236–243.
11. Price RW, Brew B, Sidtis J, Rosenblum M, Scheck AC, Cleary P. **The brain in AIDS: central nervous system HIV-1 infection and AIDS dementia complex.** *Science* 1988; **239**:586–592.
12. Ances BM, Roc AC, Wang J, Korczykowski M, Okawa J, Stern J, *et al*. **Caudate blood flow and volume are reduced in HIV+ neurocognitively impaired patients.** *Neurology* 2006; **66**:862–866.
13. Ances BM, Ortega M, Vaida F, Heaps J, Paul R. **Independent effects of HIV, aging, and HAART on brain volumetric measures.** *J Acquir Immune Defic Syndr* 2012; **59**:469–477.
14. Antinori A, Coenen T, Costagiola D, Dedes N, Ellefson M, Gatell J, *et al*. **Late presentation of HIV infection: a consensus definition.** *HIV Med* 2011; **12**:61–64.
15. Hammoud DA, Boulougoura A, Papadakis GZ, Wang J, Dodd LE, Rupert A, *et al*. **Increased metabolic activity on 18F-fluorodeoxyglucose positron emission tomography-computed tomography in human immunodeficiency virus-associated immune reconstitution inflammatory syndrome.** *Clin Infect Dis* 2019; **68**:229–238.
16. Hammoud DA, Sinharay S, Steinbach S, Wakim PG, Geannopoulos K, Traino K, *et al*. **Global and regional brain hypometabolism on FDG-PET in treated HIV-infected individuals.** *Neurology* 2018; **91**:e1591–e1601.
17. Yang J, Hu C, Guo N, Dutta J, Vaina LM, Johnson KA, *et al*. **Partial volume correction for PET quantification and its impact on brain network in Alzheimer's disease.** *Sci Rep* 2017; **7**:13035.
18. Kallianpur KJ, Jahanshad N, Sailasuta N, Benjapornpong K, Chan P, Pothisri M, *et al*. **Regional brain volumetric changes despite two years of treatment initiated during acute HIV infection.** *AIDS* 2020; **34**:415–426.
19. Wang GJ, Volkow ND, Wolf AP, Brodie JD, Hitzemann RJ. **Intersubject variability of brain glucose metabolic measurements in young normal males.** *J Nucl Med* 1994; **35**:1457–1466.
20. Bakdash JZ, Marusich LR. **Repeated measures correlation.** *Front Psychol* 2017; **8**:456.
21. Gisslen M, Fuchs D, Svennerholm B, Hagberg L. **Cerebrospinal fluid viral load, intrathecal immunoactivation, and cerebrospinal fluid monocytic cell count in HIV-1 infection.** *J Acquir Immune Defic Syndr* 1999; **21**:271–276.
22. Kim WK, Avarez X, Williams K. **The role of monocytes and perivascular macrophages in HIV and SIV neuropathogenesis: information from nonhuman primate models.** *Neurotox Res* 2005; **8**:107–115.
23. Castley A, Berry C, French M, Fernandez S, Krueger R, Nolan D. **Elevated plasma soluble CD14 and skewed CD16+ monocyte distribution persist despite normalisation of soluble CD163 and CXCL10 by effective HIV therapy: a changing paradigm for routine HIV laboratory monitoring?** *PLoS One* 2014; **9**:e115226.
24. Shive CL, Jiang W, Anthony DD, Lederman MM. **Soluble CD14 is a nonspecific marker of monocyte activation.** *AIDS* 2015; **29**:1263–1265.
25. Williams JC, Zhang X, Karki M, Chi YY, Wallet SM, Rudy BJ, *et al*. **Soluble CD14, CD163, and CD27 biomarkers distinguish ART-suppressed youth living with HIV from healthy controls.** *J Leukoc Biol* 2018; **103**:671–680.
26. Sereti I, Krebs SJ, Phanuphak N, Fletcher JL, Slike B, Pinyakorn S, *et al*. **Persistent, albeit reduced, chronic inflammation in persons starting antiretroviral therapy in acute HIV infection.** *Clin Infect Dis* 2017; **64**:124–131.
27. Sandler NG, Wand H, Roque A, Law M, Nason MC, Nixon DE, *et al*. **Plasma levels of soluble CD14 independently predict mortality in HIV infection.** *J Infect Dis* 2011; **203**:780–790.
28. Ryan LA, Zheng J, Brester M, Bohac D, Hahn F, Anderson J, *et al*. **Plasma levels of soluble CD14 and tumor necrosis factor-alpha type II receptor correlate with cognitive dysfunction during human immunodeficiency virus type 1 infection.** *J Infect Dis* 2001; **184**:699–706.
29. Imp BM, Rubin LH, Tien PC, Plankey MW, Golub ET, French AL, *et al*. **Monocyte activation is associated with worse cognitive performance in HIV-infected women with virologic suppression.** *J Infect Dis* 2017; **215**:114–121.
30. Munoz-Nevarez LA, Imp BM, Eller MA, Kiweewa F, Maswai J, Polyak C, *et al*. **Monocyte activation, HIV, and cognitive performance in East Africa.** *J Neurovirol* 2019; **26**:52–59.
31. Kamkwalala AR, Wang X, Maki PM, Williams DW, Valcour VG, Damron A, *et al*. **Higher peripheral monocyte activation markers are associated with smaller frontal and temporal cortical volumes in women with HIV.** *J Acquir Immune Defic Syndr* 2020; **84**:54–59.
32. Sanford R, Ances BM, Meyerhoff DJ, Price RW, Fuchs D, Zetterberg H, *et al*. **Longitudinal trajectories of brain volume and cortical thickness in treated and untreated primary human immunodeficiency virus infection.** *Clin Infect Dis* 2018; **67**:1697–1704.
33. Gonzalez-Scarano F, Martin-Garcia J. **The neuropathogenesis of AIDS.** *Nat Rev Immunol* 2005; **5**:69–81.
34. Andersen AB, Law I, Krabbe KS, Bruunsgaard H, Ostrowski SR, Ullum H, *et al*. **Cerebral FDG-PET scanning abnormalities in optimally treated HIV patients.** *J Neuroinflammation* 2010; **7**:13.
35. Alakkas A, Ellis RJ, Watson CW, Umlauf A, Heaton RK, Letendre S, *et al*. **White matter damage, neuroinflammation, and neuronal integrity in HAND.** *J Neurovirol* 2019; **25**:32–41.
36. Neuen-Jacob E, Arendt G, Wendtland B, Jacob B, Schneeweis M, Wechsler W. **Frequency and topographical distribution of CD68-positive macrophages and HIV-1 core proteins in HIV-associated brain lesions.** *Clin Neuropathol* 1993; **12**:315–324.

37. Brew BJ, Rosenblum M, Cronin K, Price RW. **AIDS dementia complex and HIV-1 brain infection: clinical-virological correlations.** *Ann Neurol* 1995; **38**:563–570.
38. Lee DE, Reid WC, Ibrahim WG, Peterson KL, Lentz MR, Maric D, *et al*. **Imaging dopaminergic dysfunction as a surrogate marker of neuropathology in a small-animal model of HIV.** *Mol Imaging* 2014; **13**:9.
39. Shah S, Maric D, Denaro F, Ibrahim W, Mason R, Kumar A, *et al*. **Nitrosative stress is associated with dopaminergic dysfunction in the HIV-1 transgenic rat.** *Am J Pathol* 2019; **189**:1375–1385.
40. Sinharay S, Hammoud DA. **Brain PET imaging: value for understanding the pathophysiology of HIV-associated neurocognitive disorder (HAND).** *Curr HIV/AIDS Rep* 2019; **16**:66–75.
41. Sinharay S, Lee D, Shah S, Muthusamy S, Papadakis GZ, Zhang X, *et al*. **Cross-sectional and longitudinal small animal PET shows pre and postsynaptic striatal dopaminergic deficits in an animal model of HIV.** *Nucl Med Biol* 2017; **55**:27–33.
42. Czub S, Czub M, Koutsilieri E, Sopper S, Villinger F, Müller JG, *et al*. **Modulation of simian immunodeficiency virus neuropathology by dopaminergic drugs.** *Acta Neuropathol* 2004; **107**:216–226.
43. Czub S, Koutsilieri E, Sopper S, Czub M, Stahl-Hennig C, Müller JG, *et al*. **Enhancement of central nervous system pathology in early simian immunodeficiency virus infection by dopaminergic drugs.** *Acta Neuropathol* 2001; **101**:85–91.
44. Gaskill PJ, Yano HH, Kalpana GV, Javitch JA, Berman JW. **Dopamine receptor activation increases HIV entry into primary human macrophages.** *PLoS One* 2014; **9**:e108232.
45. Nickoloff-Bybel EA, Mackie P, Runner K, Matt SM, Khoshbouei H, Gaskill PJ. **Dopamine increases HIV entry into macrophages by increasing calcium release via an alternative signaling pathway.** *Brain Behav Immun* 2019; **82**:239–252.
46. Rottenberg DA, Moeller JR, Strother SC, Sidtis JJ, Navia BA, Dhawan V, *et al*. **The metabolic pathology of the AIDS dementia complex.** *Ann Neurol* 1987; **22**:700–706.
47. Hinkin CH, van Gorp WG, Mandelkern MA, Gee M, Satz P, Holston S, *et al*. **Cerebral metabolic change in patients with AIDS: report of a six-month follow-up using positron-emission tomography.** *J Neuropsychiatry Clin Neurosci* 1995; **7**:180–187.
48. Rottenberg DA, Sidtis JJ, Strother SC, Schaper KA, Anderson JR, Nelson MJ, *et al*. **Abnormal cerebral glucose metabolism in HIV-1 seropositive subjects with and without dementia.** *J Nucl Med* 1996; **37**:1133–1141.
49. von Giesen HJ, Antke C, Hefter H, Wenserski F, Seitz RJ, Arendt G. **Potential time course of human immunodeficiency virus type 1-associated minor motor deficits: electrophysiologic and positron emission tomography findings.** *Arch Neurol* 2000; **57**:1601–1607.
50. Yoshizawa H, Gazes Y, Stern Y, Miyata Y, Uchiyama S. **Characterizing the normative profile of 18F-FDG PET brain imaging: sex difference, aging effect, and cognitive reserve.** *Psychiatry Res* 2014; **221**:78–85.
51. Ellis RJ, Badiee J, Vaida F, Letendre S, Heaton RK, Clifford D, *et al*. **CD4 nadir is a predictor of HIV neurocognitive impairment in the era of combination antiretroviral therapy.** *AIDS* 2011; **25**:1747–1751.
52. Thompson MA, Aberg JA, Hoy JF, Telenti A, Benson C, Cahn P, *et al*. **Antiretroviral treatment of adult HIV infection: 2012 recommendations of the International Antiviral Society-USA panel.** *JAMA* 2012; **308**:387–402.
53. Han H, Agarwal R, Martel-Laferriere V, Dieterich DT. **Antiretroviral and antihepatitis C virus direct-acting antiviral-related hepatotoxicity.** *Clin Liver Dis* 2013; **17**:657–670ix.